JACS ARTICLES

Published on Web 11/10/2010

Kinetics of Ion Transfer at the Ionic Liquid/Water Nanointerface

Yixian Wang,[†] Takashi Kakiuchi,[‡] Yukinori Yasui,[‡] and Michael V. Mirkin*,[†]

Department of Chemistry and Biochemistry, Queens College − CUNY, Flushing, New York 11367, United States, and Department of Energy and Hydrocarbon Chemistry, Graduate School of Engineering, Kyoto University, Kyoto 615-8510, Japan

Received August 5, 2010; E-mail: mmirkin@qc.cuny.edu

Abstract: Ion transfer (IT) processes in ionic liquids (ILs) are essential for their applications in electrochemical systems and chemical separations. In this Article, the first measurements of IT kinetics at the IL/water interface are reported. Steady-state voltammetry was performed at the nanometer-sized polarizable interface between water and ionic liquid, $[THTDP^+][C_4C_4N^-]$, immiscible with it that was formed at the tip of a nanopipet. Kinetic measurements at such interfaces are extremely challenging because of slow mass-transfer rates in IL, which is ~700 times more viscous than water. The recently developed new mode of nanopipet voltammetry, common ion voltammetry, was used to overcome technical difficulties and ensure the reliability of the extracted kinetic parameters of IT. The results suggest that the rate of interfacial IT depends strongly on solution viscosity. Voltammetric responses of nanopipets of different radii were analyzed to evaluate the effect of the electrical double layer at the liquid/liquid interface on IT kinetics. The possibility of the influence of the charged pipet wall on ion transport was investigated by comparing currents produced by cationic and anionic species. Possible effects of relaxation phenomena at the IL/water interface on IT voltammograms have also been explored.

Introduction

Ion transfer (IT) reactions at the water/ionic liquid (IL) interface are central to a growing number of useful applications of ILs, for example, in fuel cells, sensors, and solvent extraction.[1−3] Although a number of theoretical and experimental studies of IL electrochemistry have been reported,[4] to our knowledge, the kinetics of IT reactions have not yet been measured. Many fundamental questions in this area remain open including the double layer structure in ionic liquids and its effects on IT, the applicability of existing IT theory, and the dynamics of the responses of the IL/water interface to the applied voltage.[5−9]

In all previous studies of IT at the interface between two immiscible electrolyte solutions (ITIES), the two liquid phases were water and an organic solvent.[10] The unique structural and physicochemical properties of ILs (e.g., viscosity, conductivity, and solvation) offer an opportunity to study dynamics of interfacial IT reactions in a system substantially different from conventional ITIES. Two main obstacles hindering electrochemical studies of ITs at the water/IL interface are the difficulties in obtaining a sufficiently wide polarization window and slow mass transfer in ILs. Our previous electron transfer studies were carried out at a nonpolarizable IL/water interface, where the width of a polarization window was not an issue.[7] For IT studies at a polarizable IL/water interface, one needs highly hydrophobic ILs, which became available only a few years ago.[11] Such ILs are typically much more viscous than water or regular organic solvents, thus giving us a chance to investigate a largely unexplored effect of viscosity on the IT rate at the liquid/liquid interface. For instance, trihexyltetradecylphosphonium bis(1,1,2,2,3,3,4,4,4-nonafluoro-1-butanesulfonyl)imide ($[THTDP^+][C_4C_4N^-]$) employed in our study yielded voltammograms with low background current and good polarization window (>400 mV); however, slow diffusion in this

[†] Queens College.
[‡] Kyoto University.

(1) MacFarlane, D. R.; Forsyth, M.; Howlett, P. C.; Pringle, J. M.; Sun, J.; Annat, G.; Neil, W.; Izgorodina, E. I. *Acc. Chem. Res.* **2007**, *40*, 1165.
(2) Han, X.; Armstrong, D. W. *Acc. Chem. Res.* **2007**, *40*, 1079.
(3) *Electrochemical Aspects of Ionic Liquids*; Ohno, H., Ed.; Wiley: Hoboken, 2005.
(4) Hapiot, P.; Lagrost, C. *Chem. Rev.* **2008**, *108*, 2238.
(5) (a) Kornyshev, A. A. *J. Phys. Chem. B* **2007**, *111*, 5545. (b) Fedorov, M. V.; Kornyshev, A. A. *Electrochim. Acta* **2008**, *53*, 6835. (c) Fedorov, M. V.; Kornyshev, A. A. *J. Phys. Chem. B* **2008**, *112*, 11868.
(6) Islam, M. M.; Alam, M. T.; Okajima, T.; Ohsaka, T. *J. Phys. Chem. C* **2009**, *113*, 3386.
(7) (a) Laforge, F. O.; Kakiuchi, T.; Shigematsu, F.; Mirkin, M. V. *J. Am. Chem. Soc.* **2004**, *126*, 15380. (b) Laforge, F. O.; Kakiuchi, T.; Shigematsu, F.; Mirkin, M. V. *Langmuir* **2006**, *22*, 10705.
(8) Nishi, N.; Murakami, H.; Imakura, S.; Kakiuchi, T. *Anal. Chem.* **2006**, *78*, 5805.
(9) (a) Yasui, Y.; Kitazumi, Y.; Ishimatsu, R.; Nishi, N.; Kakiuchi, T. *J. Phys. Chem. B* **2009**, *113*, 3273. (b) Kakiuchi, T.; Yasui, Y.; Kitazumi, Y.; Nishi, N. *ChemPhysChem* **2010**, *11*, 2912.
(10) For a review of IT processes at the ITIES, see: (a) Girault, H. H. In *Modern Aspects of Electrochemistry*; Bockris, J. O'M., Conway, B. E., White, R. E., Eds.; Plenum Press: New York, 1993; Vol. 25, p 1. (b) Vaňýsek, P. In *Biomembrane Electrochemistry*; Blank, M., Vodyanoy, I., Eds.; American Chemical Society: Washington, DC, 1994; p 55. (c) Samec, Z.; Kakiuchi, T. In *Advances in Electrochemical Science and Electrochemical Engineering*; Gerischer, H., Tobias, C. W., Eds.; VCH: New York, 1995; Vol. 4, p 297. (d) Dryfe, R. A. W. *Advances in Chemical Physics*; Wiley-Interscience: New York, 2009; Vol. 141, p 153.
(11) Nishi, N.; Imakura, S.; Kakiuchi, T. *Anal. Chem.* **2006**, *78*, 2726.

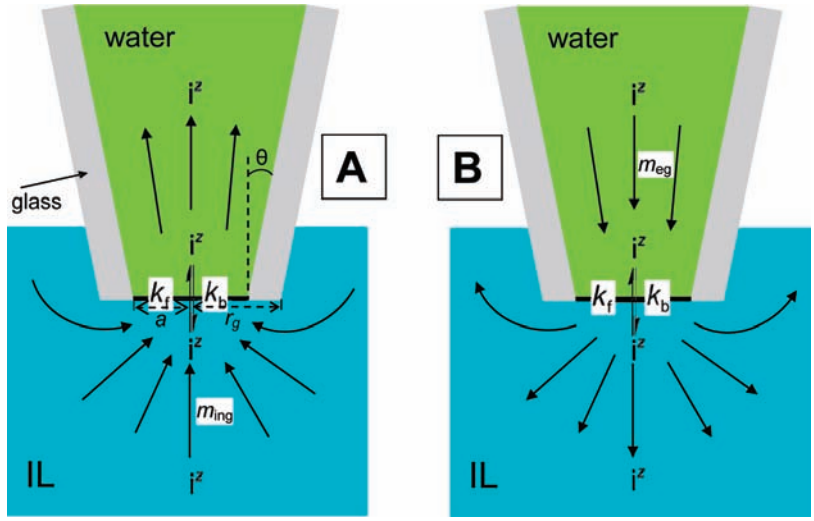

Figure 1. Scheme of simple IT at a nanopipet-supported ITIES showing the transfer of i^z ion from the external IL solution to the aqueous filling solution (A) and the reverse process (B).

viscous IL resulted in very small diffusion currents at nanopipets and other challenges in determination of fast interfacial IT kinetics.

The heterogeneous kinetics can be measured by an electrochemical method only if the mass-transfer coefficient (m) is not much smaller than the standard rate constant ($k°$). Generally, $k° \geq 10m$ corresponds to essentially diffusion-controlled (Nernstian) charge transfer reaction.[12] Rapid IT kinetics were previously studied at water/organic solvent interfaces formed at the tip of a nanometer-sized pipet to ensure a sufficiently high rate of mass transfer.[13−18] When an ion is transferred from the external liquid phase (here, it is IL; Figure 1A) to the filling solution inside the pipet (water), the steady-state diffusion limiting current (i_{ing}, i.e., ingress current) and the corresponding mass-transfer coefficient, (m_{ing}) are

$$i_{ing} = 4xzFD_{IL}c_{IL}a \quad (1)$$

and

$$m_{ing} = \frac{4xD_{IL}}{\pi a} \quad (2)$$

where z, D_{IL}, and c_{IL} are the charge of the transferred ion, its diffusion coefficient, and bulk concentration in the external solution, respectively, a is the pipet radius, and x is a function of r_g/a (r_g is the outer wall radius; $r_g/a \cong 1.5$; and $x = 1.16$ for typical borosilicate pipets).[18]

Because of the asymmetry of the diffusion field at a pipet-based ITIES, where the diffusion inside a cylindrical shaft is quasi-linear in contrast to the spherical diffusion of ions to the pipet orifice in the external IL solution, an IT voltammogram at a micrometer-sized ITIES consists of a steady-state, sigmoidal ingress wave and a time-dependent, peak-shaped wave produced by the reverse reaction (i.e., egress of the same ion to the external solution; Figure 1B).[19] The egress IT can reach a steady-state if the pipet orifice is sufficiently small ($a \ll 1\ \mu$m) and the potential sweep rate is not fast (e.g., a few mV/s).[16,20] Under these conditions, the steady-state diffusion limiting egress current, i_{eg}, and the corresponding mass-transfer coefficient, m_{eg}, are given by eqs 3 and 4:[21]

$$i_{eg} = 4f(\theta)z_iFD_wc_wa \quad (3)$$

$$m_{eg} = \frac{4f(\theta)D_w}{\pi a} \quad (4)$$

where D_w and c_w are the diffusion coefficient and bulk concentration in the internal aqueous solution, respectively, and $f(\theta)$ is a tabulated function of the tip taper angle, θ.[18,21]

In earlier studies, it was assumed that a steady-state response produced by ingress IT is essentially independent of the ion transport inside the pipet.[16,19] However, recent simulations showed that geometry of the pipet inside can significantly affect IT voltammograms.[21−23] Additionally, it was found that an experimental voltammogram of rapid (near-Nernstian) IT obtained with a transferable ion present only in one liquid phase (i.e., either in the external (Figure 1A) or in the internal (Figure 1B) solution) can be fit to the theory using different combinations of kinetic parameters.[24] The unavailability of the unique fit can lead to large uncertainties in kinetic parameters (i.e., $k°$ and the transfer coefficient, α)

(12) (a) Bard, A. J.; Faulkner, L. R. *Electrochemical Methods: Fundamentals and Applications*, 2nd ed.; Wiley & Sons: New York, 2001. (b) Mirkin, M. V.; Bard, A. J. *Anal. Chem.* **1992**, *64*, 2293.
(13) Shao, Y.; Mirkin, M. V. *J. Am. Chem. Soc.* **1997**, *119*, 8103.
(14) Yuan, Y.; Shao, Y. H. *J. Phys. Chem. B* **2002**, *106*, 7809.
(15) Jing, P.; Zhang, M. Q.; Hu, H.; Xu, X. D.; Liang, Z. W.; Li, B.; Shen, L.; Xie, S. B.; Pereira, C. M.; Shao, Y. H. *Angew. Chem., Int. Ed.* **2006**, *45*, 6861.
(16) Cai, C. X.; Tong, Y. H.; Mirkin, M. V. *J. Phys. Chem. B* **2004**, *108*, 17872.
(17) Li, Q.; Xie, S.; Liang, Z.; Meng, X.; Liu, S.; Girault, H. H.; Shao, Y. *Angew. Chem., Int. Ed.* **2009**, *48*, 8010.
(18) Wang, Y.; Velmurugan, J.; Mirkin, M. V.; Rodgers, P. J.; Kim, J.; Amemiya, S. *Anal. Chem.* **2010**, *82*, 77.
(19) Stewart, A. A.; Taylor, G.; Girault, H. H.; McAleer, J. *J. Electroanal. Chem.* **1990**, *296*, 491.
(20) Tong, Y.; Shao, Y.; Wang, E. *Anal. Chem. (in Chin.)* **2001**, *11*, 1241.
(21) Rodgers, P. J.; Amemiya, S. *Anal. Chem.* **2007**, *79*, 9276.
(22) Tsujioka, N.; Imakura, S.; Nishi, N.; Kakiuchi, T. *Anal. Sci.* **2006**, *22*, 667.
(23) Nishi, N.; Imakura, S.; Kakiuchi, T. *J. Electroanal. Chem.* **2008**, *621*, 297.
(24) Rodgers, P. J.; Amemiya, S.; Wang, Y.; Mirkin, M. V. *Anal. Chem.* **2010**, *82*, 84.

extracted from such voltammograms. The accuracy and precision of IT kinetic measurements can be greatly improved by using common ion voltammetry, in which a transferable ion is added to both immiscible liquid phases.[18,24] The advantages of common ion voltammetry stem from the availability of two waves corresponding to the ingress of the common ion into the pipet (Figure 1A) and its egress to the external solution (Figure 1B). From two limiting currents of a single voltammogram, one can assess asymmetric ion diffusion in the internal and external solutions and evaluate the related geometric and transport parameters using eqs 1−4. Moreover, the unique combination of kinetic parameters can be found by fitting an experimental voltammogram to the theory expressed by eq 5:[24]

$$\frac{i}{i_{ing}} = \frac{1}{m_{ing}/m_{eg} + m_{ing}/k_b + k_f/k_b}\left(\frac{k_f}{k_b} - \frac{c_w}{c_{IL}}\right) \quad (5)$$

k_f and k_b in eq 5 are the heterogeneous rate constants given by the Butler−Volmer-type model:

$$k_f = k^0 \exp\left[\frac{-\alpha z_i F(\Delta\phi - \Delta\phi_i^{0'})}{RT}\right] \quad (6a)$$

$$k_b = k^0 \exp\left[\frac{(1-\alpha) z_i F(\Delta\phi - \Delta\phi_i^{0'})}{RT}\right] \quad (6b)$$

where $\Delta\phi$ is the Galvani potential difference between two liquid phases and $\Delta\phi_i^{0'}$ is the formal transfer potential of ion i. The precision is further enhanced by separate determination of $\Delta\phi_i^{0'}$ from the potential value at zero current, $\Delta\phi_{eq}$, in a nanopipet voltammogram:

$$\Delta\phi_{eq} = \Delta\phi_i^{0'} + \frac{RT}{z_i F}\ln\frac{c_{IL}}{c_w} \quad (7)$$

In studies at the water/organic solvent interface, the diffusion coefficients of the trasferable ion in both phases were of the same order of magnitude, and m_{ing} was typically several times larger than m_{eg} because radial diffusion of ions to the tip in the external solution is much less hindered by the pipet wall.[18,21] In contrast, at the water/IL interface, $D_{IL} \ll D_w$ and consequently $m_{ing} \ll m_{eg}$. Different extents of reversibility (i.e., kinetic vs diffusion control) of the ion ingress and egress processes can be assessed using two dimensionless parameters, $\lambda_{ing} = k^0/m_{ing}$ and $\lambda_{eg} = k^0/m_{eg}$. Here, we explore this unusual situation and show that common ion voltammetry can be used to investigate the kinetics of such IT processes.

Experimental Section

Chemicals. The following chemicals were used as received: LiCl, $MgSO_4$, 1-methyl-3-octylimidazolium chloride (C_8mimCl), and chlorotrimethylsilane from Aldrich; tetraethylammonium chloride (TEACl) from Sigma; potassium tetrakis(4-chlorophenyl)borate (KTPBCl), tetrabutylammonium chloride (TBACl), tetrahexylammonium chloride (THACl), and tetrabutylammonium perchlorate ($TBAClO_4$) from Fluka. 1,2-Dichloethane (DCE) from Sigma was distilled once. Tetrabutylammonium tetrakis(4-chlorophenyl)borate (TEATPBCl) and tetrahexylammonium tetrakis(4-chlorophenyl)borate (THATPBCl) were prepared by metathesis of KTPBCl with TEACl and THACl, respectively, as described previously.[25] The ionic liquids, trihexyltetradecylphosphonium bis(1,1,2,2,3,3,4,4,4-nonafluoro-1-butanesulfonyl)imide ($[THTDP^+][C_4C_4N^-]$) and 1-methyl-3-octylimidazolium bis(pentafluoroethylesufonyl)imide ($[C_8mim^+][C_2C_2N^-]$), were synthesized by the Kakiuchi group at Kyoto University. Tetrabutylammonium bis(1,1,2,2,3,3,4,4,4-nonafluoro-1-butanesulfonyl)imide ($TBA[C_4C_4N^-]$) was prepared by metathesis of HC_4C_4N and TBACl. All aqueous solutions were prepared from deionized water (Milli-Q, Millipore Corp.).

Nanopipet Preparation. The nanopipets (with radii from 10 to 150 nm) were made from 15 cm long borosilicate capillaries (outer/inner diameter ratio of 1.0/0.58 mm; Sutter Instrument Co., Novato, CA), using a laser-based pipet puller (P-2000G, Sutter Instrument Co.), as described previously.[13,16,18] The pipets were filled with aqueous solution from the rear, using a small (10 μL) syringe. A reference electrode was inserted into each pipet from the rear.

The outer glass wall of a pipet was silanized in the vapor of chlorotrimethylsilane to render it hydrophobic, which was done by holding the pipet 1−2 cm above the liquid surface of the reagent for ∼30 s, while the flow of argon was passed through the pipet from the back. The required silanization time depends on the distance between the chlorotrimethylsilane surface and the pipet, its radius, and room temperature.

Voltammetry of TBA^+ or C_8mim^+ as a common ion was used to characterize silanized and nonsilanized nanopipets, as discussed previously.[18] A pair of pipets with the same radius was pulled from the same borosilicate capillary to compare the responses of silanized and nonsilanized nanopipets.

Instrumentation. A BAS 100B electrochemical workstation (Bioanalytical Systems, West Lafayette, IN) was employed to record the cyclic voltammograms. An Olympus BH2 optical microscope (100× to 500× magnification) was used to inspect all prepared pipets before measurements.

Voltammetric Measurements. Voltammetric experiments were carried out at room temperature (23 ± 2 °C) in a two-electrode U-tube cell. The voltage was applied between two aqueous reference electrodes. Both of them were 0.25 mm diameter Ag wires coated with either AgCl or Ag_2SO_4, as follows:

$$\underset{\text{Aqueous reference}}{Ag|AgCl|0.1\text{ M LiCl} + 0.1\text{ M } HC_4C_4N} \,||\, \underset{[THTDP^+][C_4C_4N^-]}{c_{IL}\text{ mM } TBA[C_4C_4N^-]} \,||\, \underset{\text{Pipet}}{30\text{ mM } MgSO_4 + c_w\text{ mM TBACl}|Ag_2SO_4|Ag} \quad \text{(cell1)}$$

or

$$\underset{\text{Aqueous reference}}{Ag|AgCl|0.1\text{ M LiCl} + 0.1\text{ M } HC_4C_4N} \,||\, \underset{[THTDP^+][C_4C_4N^-]}{c_{IL}\text{ mM}[C_8mim^+][C_2C_2N^-]} \,||\, \underset{\text{Pipet}}{0.1\text{ M LiCl} + c_w\text{ mM } C_8mimCl|AgCl|Ag} \quad \text{(cell2)}$$

or

$$\underset{\text{Aqueous reference}}{Ag|AgCl|0.1\text{ M LiCl} + 0.1\text{ M } HC_4C_4N} \,||\, \underset{[THTDP^+][C_4C_4N^-]}{c_{IL}\text{ mM } TBA[C_4C_4N^-]} \,||\, \underset{\text{Pipet}}{0.1\text{ M LiCl} + c_w\text{ mM } TBAClO_4|AgCl|Ag} \quad \text{(cell3)}$$

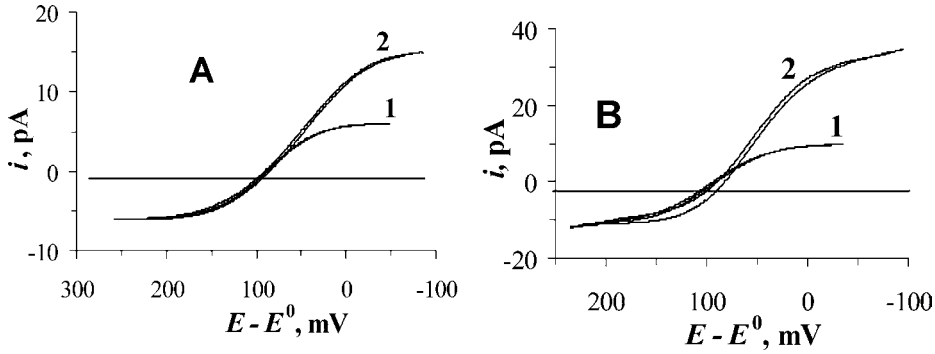

Figure 2. CVs of TBA^+ (A) and C_8mim^+(B) transfers across the IL/water interfaces obtained with silanized (1) and nonsilanized (2) nanopipets pulled from the same capillaries. *a*, nm = 82 (A) and 60 (B). The CVs were obtained in cell 1 with $c_w = 3.1$ mM and $c_{IL} = 93$ mM (A), and in cell 2 with $c_w = 5.0$ mM and $c_{IL} = 170$ mM (B). ν, mV/s = 1 (1) and 10 (2).

The current produced by the cation transfer from the outer IL phase to the aqueous filling solution was designated as positive.

Results and Discussion

Silanization of Nanopipets. A water-filled pipet has to be silanized before it is immersed in an organic solution to eliminate a thin aqueous film that otherwise forms on its hydrophilic outer wall making the true area of the liquid/liquid interface much larger than the geometrical area of the pipet orifice.[26] High-resolution SEM showed that silanization results in a formation of a nanometer-thick film on the pipet wall.[24] Although such a film does not significantly affect the response of a relatively large (e.g., ≥100 nm) pipet, silanization of smaller pipets must be done cautiously to avoid the formation of a thicker film, which can partially block the pipet orifice and induce solvent penetration into its narrow shaft. A recently developed protocol for silanizing pipets in the vapor phase allows one to avoid oversilanization of relatively small (e.g., ≥10 nm radius) pipets.[24] We used the same approach here and found that proper silanization of borosilicate pipets for measurements in IL can be achieved with a shorter exposure time of ~30 s. In this way, one can further decrease the chances of oversilanizing relatively small pipets required for kinetic experiments at the IL/water interface.

The effect of silanization was evaluated by comparing the diffusion limiting current recorded at a silanized and nonsilanized pipets pulled from the same glass capillary. Voltammograms obtained in cell 1 at silanized (curve 1) and nonsilanized (curve 2) pipets show TBA^+ egress and ingress waves (Figure 2A). Both waves are sigmoidal, thereby confirming steady-state diffusion of TBA^+ on both sides of the nanoscale interface. The positive limiting current produced by the ingress of TBA^+ at the nonsilanized pipet is ~2.5 times larger than that at the silanized nanopipet; this value is in a good agreement with the theoretically expected ratio of $3.35\pi/(4 \times 1.16) = 2.3$.[16,26] Unlike i_{ing}, the egress current should not be affected by silanization if the orifice radius does not change;[18] this kind of behavior can be seen in Figure 2A. Similar effects of silanization on the voltammograms of the transfer of a different, asymmetric C_8mim^+ ion at the water/IL nanointerface (cell 2) can be seen in Figure 2B.

To obtain similar i_{eg} and i_{ing} in Figure 2, the concentration of the common ion in IL had to be >30 times its value in the filling aqueous solution because of much slower diffusion in IL (see below). Such high concentrations were attainable because of high solubilities of both $TBA[C_4C_4N^-]$ and $[C_8mim^+][C_2C_2N^-]$ in $[THTDP^+][C_4C_4N^-]$, and the contribution of migration to the mass transfer remained negligible because of high ionic concentrations in IL. Another issue related to slow diffusion is the time required to attain a steady-state.[27] Using 1-methyl-3-octylimidazolium-bis(tetrafluoromethylsulfonyl)imide (C_8mim-C_1C_1N) IL, a steady-state at nanopipet-supported ITIES could be reached on a millisecond time scale.[28] In more viscous $[THTDP^+][C_4C_4N^-]$, the mass transfer is even slower, and retraceable steady-state voltammograms can be obtained only at a very slow scan rate. For example, voltammograms obtained at the scan rate, $\nu = 10$ mV/s (curves 2 in Figure 2), are not perfectly retraceable unlike those recorded with $\nu = 1$ mV/s (curves 1 in Figure 2). Kinetic measurements at nanopipet-supported ITIES have to be done under steady-state conditions because the detailed picture of the pipet inside geometry required for theoretical treatment of nonsteady-state responses is not available.

Diffusion Coefficients of Ions in IL. The diffusion coefficient of TBA^+ in IL can be determined from the steady-state diffusion limiting current to a nanopipet orifice using eq 1. To minimize the uncertainty associated with the values of *x* and *a* for a nanopipet, D_{IL} was determined from the ratio of the diffusion limiting currents measured at the same pipet in IL and in DCE solution. In the latter case, the transferred ion was TEA^+, $z_{DCE} = z_{IL} = 1$, and thus

$$i_{ing,IL}/i_{ing,\,DCE} = D_{IL}c_{IL}/D_{DCE}c_{DCE} \tag{8}$$

and

$$\frac{D_{IL}}{D_{DCE}} = \frac{i_{ing,IL}}{i_{ing,DCE}}\frac{c_{DCE}}{c_{IL}} \tag{9}$$

After measuring $i_{ing,IL}$ in cell 1 with $c_w = 0$ and $c_{IL} = 293$ mM, a silanized pipet was transferred to DCE phase containing $c_{DCE} = 0.4$ mM of TEA^+ to obtain a steady-state voltammogram and determine $i_{ing,DCE}$. In this way, the D_{IL}/D_{DCE} ratio was found using several pipets with different radii (Table 1). With $D_{DCE,TEA} = 9.8 \times 10^{-6}$ cm^2/s,[16] the data in Table 1 yield $D_{IL,TBA} = (2.0_3 \pm 0.1_6) \times 10^{-8}$ cm^2/s. This value is ~275 times lower than the diffusion coefficient of TBA in water (5.5×10^{-6} cm^2/s[29]).

(25) Shao, Y.; Girault, H. H. *J. Electroanal. Chem.* **1991**, *282*, 59.
(26) Shao, Y.; Mirkin, M. V. *Anal. Chem.* **1998**, *70*, 3155.
(27) Lovelock, K. R. J.; Cowling, F. N.; Taylor, A. W.; Licence, P.; Walsh, D. A. *J. Phys. Chem. B* **2010**, *114*, 4442.
(28) Laforge, F. O.; Velmurugan, J.; Wang, Y.; Mirkin, M. V. *Anal. Chem.* **2009**, *81*, 3143.
(29) Manzanares, J. A.; Lahtinen, R.; Quinn, B.; Kontturi, K.; Schiffrin, D. J. *Electrochim. Acta* **1998**, *44*, 59.

Table 1. Determination of the Diffusion Coefficient of TBA^+ in IL

a, nm	$D_{IL,TBA}/D_{DCE,TEA} \times 10^3$
190	2.35
140	1.97
60	2.18
30	1.87
25	2.02

It was shown recently that diffusivities in IL can be significantly affected by addition of water to it.[30] To eliminate the effect of local changes in water concentration due to its dissolution at and diffusion from the ITIES into bulk IL, $[THTDP^+][C_4C_4N^-]$ used in our experiments was pre-equilibrated with water. In a similar manner, the diffusion coefficient of C_8mim^+ in IL was found from the ratio of the i_{ing} values obtained in cell 2 and cell 1 with $c_w = 0$ using differently sized pipets (from 70 nm to 1 μm radius). The determined value, $D_{IL,C8mim} = 2.0_5 \times 10^{-8}$ cm^2/s, was very similar to that of TBA^+.

Much slower diffusivities in IL (as compared to D_w) result in a significantly longer time required for the ingress IT to reach a steady-state. Two CVs in Figure 3 were obtained at a somewhat larger (500 nm radius) pipet. At $\nu = 1$ mV/s, both egress and ingress ITs in curve 1 attain a steady-state; however, at $\nu = 1$ V/s (curve 2), the egress wave remains essentially sigmoidal, while the ingress wave is peak-shaped. Conversely, conventional voltammograms at micropipets-supported ITIES exhibit a sigmoidal, steady-state ingress wave and a peak-shaped response due to egress of ions from the pipet.[19−21]

Kinetics of TBA^+ Transfer from Common Ion Voltammetry. Kinetic parameters of the TBA^+ transfer (Table 2) were extracted by fitting common ion voltammograms obtained in cell 1 to eq 5. Because of a large ratio of diffusion coefficients ($\gamma = D_w/D_{IL}$), the λ_{ing} values in the table are much larger than the corresponding λ_{eg} values; and except for pipet no. 7, all λ_{ing} values are $\geq$10. For a water/organic interface, where $\gamma \approx 1$, $\lambda_{ing} \geq 10$ corresponds to an essentially Nernstian IT process whose kinetics is too fast to measure with a given pipet. The use of smaller pipets to enhance the mass-transfer rate is not an option here because of low diffusion currents in $[THTDP^+][C_4C_4N^-]$. For example, the i_{ing} value obtained for the transfer of 93 mM TBA^+ at a 21 nm pipet (no. 7 in Table 2) was <2 pA; this is close to the lower limit for i_{ing} at which still one can obtain good quality voltammograms required for kinetic analysis. Moreover, the kinetic parameters obtained with much smaller pipets may be affected by various experimental artifacts, strong double layer effects, and deviations from the conventional electrochemical theory.[18,24,31]

Fortunately, at the water/IL interface $\gamma \gg 1$, and the reversibility limit is higher. This point is illustrated by Figure 4, where the steady-state voltammograms calculated from eq 5 for $\lambda_{ing} \geq 10$ and $\gamma = 1$ are essentially reversible (Figure 4A), while analogous curves calculated for the IL/water interface (i.e., $\gamma = 275$) are quasi-reversible as long as $\lambda \leq 50$ (Figure 4B). Accordingly, all voltammograms summarized in Table 2 are quasi-reversible (Figure 4C) except for that obtained at pipet no. 1 (Figure 4D), which is very close to the mass-transfer limit ($\lambda_{ing} = 48$). Unlike conventional IT voltammograms (i.e., those comprised either of an ingress or of an egress wave), fitting each common ion voltammogram to the theory yields a single unique combination of k^0 and α.[18,24]

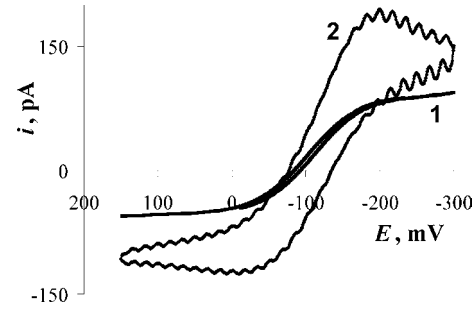

Figure 3. CVs of TBA^+ ransfer obtained in cell 1 with different scan rates. ν, mV/s = 1 (1) and 1000 (2). $a = 500$ nm. $c_w = 3.1$ mM and $c_{IL} = 93$ mM.

Importantly, there is no correlation between kinetic parameters listed in Table 2 and the pipet radius that would be indicative of double layer effects and other deviations from conventional theory. The average parameter values are $k^0 = 0.12 \pm 0.02$ cm/s and $\alpha = 0.50 \pm 0.06$. The α value of 0.5 is in agreement with the predictions of IT models either based on a concept of slow diffusion of the transferred species through the mixed interfacial layer[32,33] or assuming the existence of an activation barrier.[34,35] The determined k^0 is markedly lower than the IT rate constants measured at water/organic nanointerfaces.[13−18] For instance, it is ~50 times lower than $k^0 = 6.1$ cm/s reported recently for the transfer of TEA^+ at the water/DCE interface.[18] An obvious difference between these systems is a much higher viscosity of IL, which is likely to result in the higher viscosity of the mixed solvent layer and slower diffusion of the transferable ion through it. According to the slow interfacial diffusion model,[32,33] $k^\circ = D_i/\Delta x$, where D_i and Δx are the diffusion coefficient within the boundary layer and the thickness of that layer, respectively. One can expect D_i (and, consequently, k°) at the water/IL interface to be significantly lower than at a conventional water/organic interface; however, quantitative comparison is difficult because Δx and other factors may be different in these systems. A similar observation, that is, the IT rate constant inversely proportional to the viscosity, was made by Shao and Girault who studied the transfer of acetylcholine across the water/DCE interface and varied the viscosity by adding sucrose to the aqueous phase.[25]

In contrast, an electron transfer rate constant at the water/IL interface was higher than that measured for the same electron transfer process at the water/DCE interface.[7] One should notice that interfacial electron transfer does not involve crossing of the mixed solvent layer by any ion.

Kinetics of C_8mim^+ Transfer at the Water/IL Interface. Unlike TBA^+, C_8mim^+ is an asymmetric ion, and it is likely to adsorb at the water/IL interface. Because ionic adsorption can affect the IT rate at the ITIES,[36] we measured the kinetics of the C_8mim^+ transfer and compared it to that of TBA^+. Common ion voltammograms of the C_8mim^+ transfer at the water/

(30) (a) Schröder, U.; Wadhawan, J. D.; Compton, R. G.; Marken, F.; Suarez, P. A. Z.; Consorti, C. S.; de Souza, R. F.; Dupont, J. *New J. Chem.* **2000**, *24*, 1009. (b) Menjoge, A.; Dixon, J.; Brennecke, J. F.; Maginn, E. J.; Vasenkov, S. *J. Phys. Chem. B* **2009**, *113*, 6353.
(31) (a) Smith, C. P.; White, H. S. *Anal. Chem.* **1993**, *65*, 3343. (b) He, R.; Chen, S.; Yang, F.; Wu, B. *J. Phys. Chem. B* **2006**, *110*, 3262. (c) Liu, Y.; He, R.; Zhang, Q.; Chen, S. *J. Phys. Chem. C* **2010**, *114*, 10812.
(32) Kakiuchi, T. *J. Electroanal. Chem.* **1992**, *322*, 55.
(33) Kontturi, K.; Manzanares, J. A.; Murtomaki, L.; Schiffrin, D. J. *J. Phys. Chem.* **1997**, *101*, 10801.
(34) Schmickler, W. *J. Electroanal. Chem.* **1997**, *426*, 5.
(35) Marcus, R. A. *J. Chem. Phys.* **2000**, *113*, 1618.
(36) Nishi, N.; Izawa, K.; Yamamoto, M.; Kakiuchi, T. *J. Phys. Chem. B* **2001**, *105*, 8162.

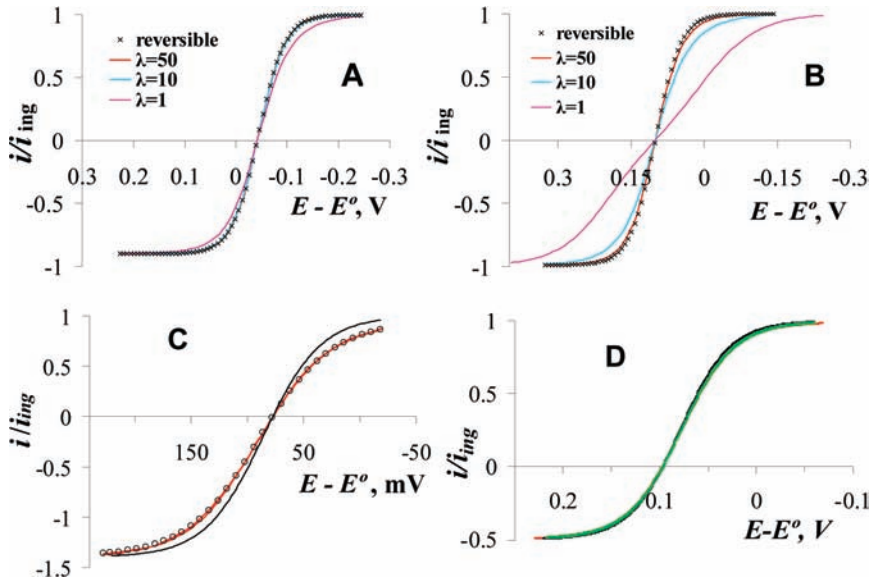

Figure 4. Kinetic analysis of steady-state common ion CVs of TBA^+ transfer across the IL/water interface. (A and B) Reversible (symbols) and quasi-reversible (solid lines) theoretical voltammograms calculated from eq 5 for $\gamma = 1$ (A) and 275 (B). $\lambda_{ing} = 1$ (pink), 10 (blue), and 50 (red). $f(\theta) = 0.21$. (C and D) Experimental CVs (red curves) fitted to the theory (black circles in (C) and green circles in (D) calculated from eq 5) with the parameter values listed for pipets no. 7 and no. 1 in Table 2, respectively. Black solid curves represent the theory for reversible IT.

Table 2. Geometric, Transport, and Kinetic Parameters Determined from Nanopipet Voltammograms of TBA^+ at the IL/Water Interface

concentrations		geometric parameters			transport parameters		kinetic parameters			
no.	c_{IL}:c_w, mM	a, nm	$f(\theta)$	θ, deg	m_{IL}, cm/s	m_w, cm/s	λ_{ing}	λ_{eg}	k^0, cm/s	α
1	93:2.1	140	0.09	6.5	0.002	0.047	48	2.2	0.10	0.57
2	93:3.1	85	0.16	11.5	0.003	0.13	38	1.0	0.13	0.43
3	93:3.1	85	0.10	8.0	0.003	0.08	32	1.4	0.11	0.59
4	93:3.1	69	0.16	11.5	0.004	0.17	19	0.5	0.08	0.52
5	123:4.4	50	0.12	9.0	0.006	0.17	30	1.0	0.18	0.43
6	141:4.6	23	0.09	6.5	0.013	0.28	10	0.5	0.13	0.54
7	93:4.6	21	0.12	9.0	0.014	0.39	6.9	0.2	0.10	0.40

Table 3. Geometric, Transport, and Kinetic Parameters Determined from Nanopipet Voltammograms of C_8mim^+ at the IL/Water Interface

concentrations		geometric parameters			transport parameters		kinetic parameters			
no.	c_{IL}:c_w, mM	a, nm	$f(\theta)$	θ, deg	m_{IL}, cm/s	m_w, cm/s	λ_{ing}	λ_{eg}	k^0, cm/s	α
1	171:5.0	66	0.18	13	0.0045	0.18	31	0.78	0.14	0.55
2	202:7.3	33	0.22	16	0.0090	0.42	17	0.36	0.15	0.47
3	202:7.4	30	0.12	9.0	0.010	0.27	18	0.66	0.18	0.50
4	202:11.6	20	0.15	11	0.015	0.52	12	0.35	0.18	0.45

$[THTDP^+][C_4C_4N^-]$ interface obtained in cell 2 (see the Supporting Information) were fitted to eq 5 to obtain kinetic parameter values listed in Table 3.

The mean value of $k^\circ = 0.16 \pm 0.02$ cm/s is only slightly larger than and $\alpha = 0.49 \pm 0.03$ is not statistically different from that found for TBA^+ transfer. The similarity of the kinetic parameters suggests that asymmetry of C_8mim^+ is not a major factor affecting the IT rate. One should also notice that the diffusion coefficients of these ions are very similar in both liquid phases.

Effect of Ionic Charge on Mass Transfer Inside the Nanopipet. The rate constants obtained at the nanometer-sized ITIES are consistently higher than those measured for the same IT reactions at larger interfaces.[10] Thus, an important question is whether the IT rates measured at the nano-ITIES, where the diffusion layer thickness is comparable to that of the diffuse double layer, can be altered by double layer effects and other size-related phenomena.[18,24,37] Possible deviations from the conventional electrochemical theory at nanointerfaces have been discussed in detail for solid nanoelectrodes.[31] Kinetic analysis of nanopipet voltammograms can be further complicated by electrostatic effects produced by the negatively charged inner glass wall.[38] The surface charge can influence ion transport along the wall electrostatically and also affect the IT rate at the edge of the nano-ITIES. Various effects of the surface charge and electrical double layer present at the inner wall including current rectification,[38] accumulation or depletion of ions near the orifice,[39] and electrostatically gated transport[40] have been investigated theoretically and experimentally for nanopipets and glass nanopore electrodes.

(37) Wang, Y.; Velmurugan, J.; Mirkin, M. V. *Isr. J. Chem* **2010**, *50*, 291.
(38) Wei, C.; Bard, A. J.; Feldberg, S. W. *Anal. Chem.* **1997**, *69*, 4627.
(39) White, H. S.; Bund, A. *Langmuir* **2008**, *24*, 2212.
(40) Wang, G.; Zhang, B.; Wayment, J. R.; Harris, J. M.; White, H. S. *J. Am. Chem. Soc.* **2006**, *128*, 7679.

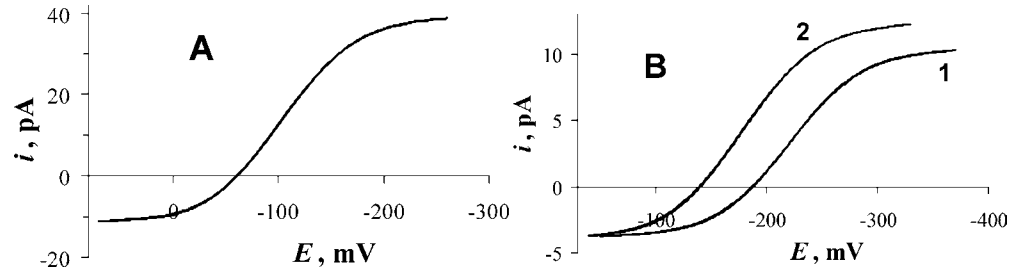

Figure 5. Steady-state CVs of ClO_4^- and TBA^+ transfers across the water/IL interface obtained in cell 3 with (A) $c_w = 13$ mM, $c_{IL} = 0$; and (B) $c_w = 10.2$ mM, $c_{IL} = 0$ (curve 1) and $c_w = 10.2$ mM, $c_{IL} = 93$ mM (curve 2). $\nu = 2$ mV/s. a, nm = 30 (A) and 11 (B).

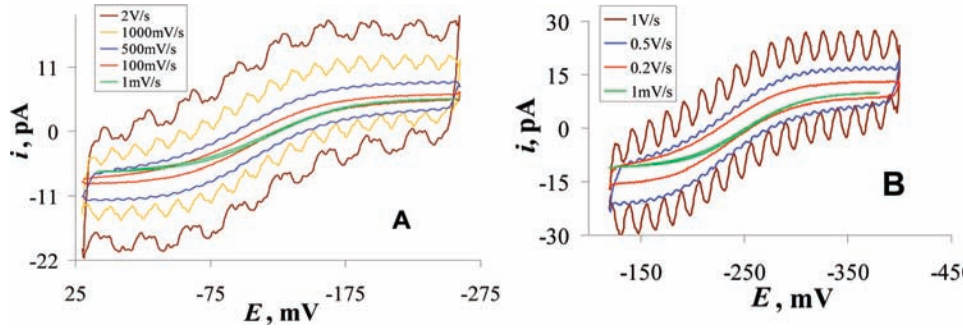

Figure 6. Effect of the potential sweep rate on CVs of IT at the water/IL interface. (A) Transfer of TBA^+ in cell 1 with $c_w = 3.1$ mM and $c_{IL} = 93$ mM. (B) Transfer of C_8mim^+ in cell 2 with $c_w = 5.0$ mM and $c_{IL} = 170$ mM. ν was varied between 1 mV/s and 2 V/s (A) and between 1 mV/s and 1 V/s (B), as shown in the color legend. $a = 60$ nm.

The absence of correlation between the measured kinetic parameters and the interfacial radius provides evidence against strong double layer effects in our experiments, where the ionic concentration was high in both phases and the pipets were not very small ($a \geq 20$ nm). To evaluate the possible influence of the charged inner wall on ion transport inside the pipet, we compared the ionic currents produced by cationic and anionic species. In Figure 5A, $TBAClO_4$ was added to the inner aqueous solution, and the IL phase contained no transferable ion (cell 3). At positive potentials applied to the pipet, TBA^+ was transferred from the filling solution to IL, and at negative potentials, perchlorate was transferred the same way. Therefore, both plateau currents in Figure 5A represent i_{eg} of ClO_4^- (positive current) and TBA^+ (negative current). These transfers occur under very similar conditions, that is, from the same pipet into the same external solution, and with identical bulk concentrations of both ions in the aqueous phase. The differences in their plateau currents can only be attributed to different diffusion coefficients and charges. The ratio of two limiting currents in the absence of electrostatic effects should be equal to D_{ClO4-}/D_{TBA+}. With $D_{TBA+} = 5.5 \times 10^{-6}$ cm^2/s[29] and $D_{ClO4-} = 1.8 \times 10^{-5}$ cm^2/s,[17] the expected current ratio is $i_{eg,ClO4-}/i_{eg,TBA+} = 3.3$ regardless of the pipet radius, that is, pretty close to the ratio of 3.5 in Figure 5A. The values obtained from several other nanopipets with different radii ranged between 3.0 and 3.6.

For a more complete analysis, after recording a voltammogram of TBA^+ and ClO_4^- transfers (curve 1 in Figure 5B), another CV was obtained with the same pipet immersed in IL containing $TBA[C_4C_4N^-]$ (curve 2 in Figure 5B). In this case, the positive plateau current was equal to $i_{eg,ClO4-} + i_{ing,TBA+}$, while the negative plateau current represented $i_{eg,TBA+}$. The difference of positive plateau currents in curves 2 and 1 equals $i_{ing,TBA+} = 12.3$ pA $- 10.3$ pA $= 2.0$ pA. Substituting this value in eq 1, one finds $a = 11$ nm. With $i_{eg,ClO4-} = 10.3$ pA, eq 3 yielded $f(\theta) = 0.13$, and $i_{eg,ClO4-}/i_{eg,TBA+} = 3.0$ was obtained from curve 1. Using nine pipets with a ranging between 11 and 250 nm, the mean value of i_{ClO4-}/i_{TBA+} was found to be 3.4. This finding and the absence of appreciable correlation between the current ratio and a suggest that electrostatic effects do not significantly influence the i_{eg} value. This finding is totally different from the results reported for nanopipets and glass nanopore electrodes immersed in an aqueous electrolyte solution (i.e., single-phase systems with no liquid/liquid interface).[38−40] One should notice that in IT voltammetry a pA-range current flowing across a nano-ITIES is much lower than that in single-phase experiments. Thus, the potential gradient and the ohmic potential drop inside the pipet are too small for significant electromigration or electroosmotic flow along its charged inner wall.[18,21]

Dynamics of Interfacial Response. We tried to detect slow relaxation phenomena recently reported at the IL/water interface[9] by investigating the effect of the potential sweep rate on the shape of IT voltammograms (Figure 6). In ref 9a, it took >1 min for the interfacial tension and the charging current to reach a steady-state after the application of a voltage across the interface between water and trioctylmethylammonium bis(nonafluorobutanesulfonyl)-amide ($[TOMA^+][C_4C_4N^-]$) IL, that is, orders of magnitude longer than the relaxation times observed at the water/organic solvent interfaces. Slow relaxation was attributed to the presence of the layered structure at the surface of IL that has been predicted by molecular dynamics simulations[41] and observed in neutron reflectivity[42] and X-ray reflectivity experiments.[43] The variation of the potential sweep rate

(41) (a) Bhargava, B. L.; Balasubramanian, S. *J. Am. Chem. Soc.* **2006**, *128*, 10073. (b) Roy, D.; Patel, N.; Conte, S.; Maroncelli, M. *J. Phys. Chem. B* **2010**, *114*, 8410.
(42) Bowers, J.; Vergara-Gutierrez, M. C.; Webster, J. R. P. *Langmuir* **2004**, *20*, 309.
(43) Mezger, M.; Schröder, H.; Reichert, H.; Schramm, S.; Okasinski, J. S.; Schöder, S.; Honkimaki, V.; Deutsch, M.; Ocko, B. M.; Ralston, J.; Rohwerder, M.; Stratmann, M.; Dosch, H. *Science* **2008**, *322*, 424.

between ~1 mV/s and 1 V/s corresponds to the change in the experimental time scale from minutes to <1 s. Such a change should significantly affect the CV shape if the IT response reflects slow interfacial dynamics. The only observable changes in the CV shape in Figure 6A caused by the increase in ν from 1 mV/s (green curve) to 2 V/s (brown curve) are a moderately higher charging current ($\leq$10 pA) and more prominent 60 Hz noise due to the decreased filtering (an automatic feature of the BAS potentiostat). The shape of CVs (i.e., the slope, the half-wave potential, and plateau currents after background subtraction) was essentially unaffected by ν, thus showing no effect of slow interfacial relaxation on IT of TBA^+.

This experiment was repeated for IT of asymmetric C_8min^+ ion, which is expected to adsorb at the liquid/liquid interface, and thus it may be a more sensitive probe for slow relaxation phenomena. However, a family of CVs in Figure 6B is quite similar to those shown in Figure 6A.

A CV obtained at $\nu = 1$ V/s shows no shift in the half-wave potential or any other features that could be attributed slow interfacial relaxation. This finding is in agreement with resent results obtained at the interface between water and trioctylmethylammonium bis(nonafluorobutanesulfonyl)-amide IL,[9b] where no slow relaxation features associated with interfacial IT were found in contrast to very slow relaxation of the electrical double layer structure observed at the same interface. This difference can be attributed to fast and slow components of the relaxation dynamics of the electrical double layer on the IL side.[9b]

Conclusions

The use of steady-state common ion voltammetry allowed us to measure IT kinetics at the nanometer-sized water/IL interfaces. These processes are hard to study because of slow mass transfer in the IL phase, which results in a low diffusion current and necessitates the use of small nanopipets and slow potential sweep rates to attain a steady-state. The measured rate constants were more than an order of magnitude lower than those obtained previously for tetraalkylammonium ions at the DCE/water interface. This difference can be attributed to higher viscosity of IL as compared to that of DCE, which should result in lower diffusivities in the interfacial mixed solvent layer. Alternatively, the decreased IT rate can be related to slower formation of the interfacial protrusions[35] (water "fingers"[44]) or different ion solvation energies in IL.[45] Very similar IT rate constants determined for TBA^+ and similarly sized but asymmetric C_8mim^+ indicate that ionic adsorption may not be a major rate-determining factor in these systems.

Despite significant differences between ILs and organic solvents, the IT responses at the IL/water interface are not strikingly different from those observed at conventional ITIES. The experimental voltammograms fit very well the theory based on Butler−Volmer model with the transfer coefficient, α, very close to 0.5. No unusual features that could be attributed to slow interfacial relaxation have been detected. Similarly, our data do not point to any "non-classical" effects of the interfacial size on IT kinetics and ion transport. The determined kinetic parameters showed no correlation with the radius of the pipet orifice for $a \geq 20$ nm. The comparison of the diffusion currents produced by the egress of cations and anions from the water-filled nanopipets ($a \geq 11$ nm) to IL showed that the mass transfer inside the pipet shaft is not significantly affected by migration and other electrostatic effects.

Acknowledgment. T.K. acknowledges the research grant (No. 21245021) from the Ministry of Education, Sports, Science, and Technology, Japan. M.V.M. acknowledges the support by the National Science Foundation (CHE-0645958 and CHE-0957313) and PSC-CUNY.

Supporting Information Available: Voltammograms of C_8mim^+ transfer at the water/IL interface. This material is available free of charge via the Internet at http://pubs.acs.org.

JA1066948

(44) Benjamin, I. *Science* **1993**, *261*, 1558.
(45) Shao, Y.; Campbell, J. A.; Girault, H. H. *J. Electroanal. Chem.* **1991**, *300*, 415.